Modeling of Magnetoelectric Antennas for Circuit Simulations in Magnetic Sensing Applications

Isabel Martos-Repath, Ankit Mittal, Mohsen Zaeimbashi, Diptashree Das, Nian X. Sun, Aatmesh Shrivastava, Marvin Onabajo

Dept. of Electrical and Computer Engineering Northeastern University, Boston, USA

{martos-repath.i, mittal.ank, zaeimbashi.m, di.das}@northeastern.edu, {nian, aatmesh, monabajo}@ece.neu.edu

Abstract — This paper introduces a behavioral circuit model for a magnetoelectric (ME) antenna, which is a novel miniaturized device with applications in low-power sensing. To facilitate the design of integrated circuits interfaced to the antenna, its model accounts for the amplitude modulation behavior observed during measurements of the nanoelectromechanical system (NEMS) device when subjected to an AC magnetic field and a DC biasing field. We propose a dynamic model for transient simulations, and show that the model characteristics match the experimentally obtained behavior of the ME antenna. As an example, the model is demonstrated through simulations of a sensor circuit for magnetic fields in the 282 microTesla to 28 milliTesla range.

Keywords — Behavioral circuit modeling, magnetoelectric antenna, sensor interface circuits, wireless medical devices.

I. Introduction

Iron-Gallium-Boron (FeGaB)-based magnetic materials have proven useful in enabling the development of compact circuit components, such as high quality factor inductors for use in radio frequency (RF) integrated circuits [1]. Magnetoelectric (ME) antennas microscale nanoelectromechanical system (NEMS) devices capable of sensing ultra-low magnitude and low-frequency magnetic fields, such as those induced by the firing of neurons in the brain [2]-[3]. They operate by utilizing a layer of FeGaB magnetostrictive material bonded to a layer of aluminum nitride (AlN) piezoelectric material, which allows the antenna to either radiate electromagnetic (EM) waves in response to an applied voltage (for transmitting), or to induce a useful voltage when exposed to an EM field (for receiving). Due to the design of the resonator elements of the ME antenna, the device exhibits dual resonant modes at different frequencies - one high (associated with its thickness, and referred to as its thin-film bulk acoustic wave resonator frequency (FBAR)), and one low (associated with its width, and referred to as its nano-plate resonator frequency (NPR)). The antenna demonstrates magnetic field sensing capability at both resonant modes, but the lower frequency mode has demonstrated better sensing performance in our past experiments. Therefore, the NPR mode may be used for sensing, whereas the FBAR mode can be utilized for other purposes such as RF energy harvesting [2], if required by the application.

These novel ME devices can potentially support a myriad of applications where sensing of low-magnitude (such as the picoTesla to milliTesla range) and low-frequency (DC to

several kilohertz) magnetic fields is required: the design of magnetometers used in unmanned aerial vehicle (UAV) navigation [4]-[5], Internet of Things (IoT) sensor platforms that can monitor electrical transmission and distribution lines [6], and wireless implantable devices [2]. Figure 1 illustrates a potential application of an ME antenna as an implantable neural activity sensor. Neural implants that use EM coupling for wireless power require either exceptionally high operating frequencies, where EM loss is very significant, or large antennas, which increase power consumption or create undesirably large implants [7]. ME antennas can be sized for sub-mm implants and operate at low frequencies to help alleviate losses due to reflection and attenuation in the layers of brain tissue [2].

For integration into implantable neuronal magnetic field (NMF) sensing devices or other applications requiring small, ultra-sensitive magnetic field detection, the ability to model ME antennas is helpful during circuit design. Previous works resulting in circuit models to describe the behavior of blood in microfluidic sensors and the building blocks of wireless communication systems for use in biometric applications have demonstrated the process and value of developing models for specific sensing applications [8]-[9]. Models, especially for systems with blocks that require an interface with an antenna, enable the use of co-design as a methodology [10]-[11]. Having a behavioral circuit model for ME antennas enables the co-design of other crucial circuits. such as oscillators and amplifiers, during the development of more complex systems for sensing applications. This paper proposes the first such ME antenna model, as well as exemplifies a neuronal magnetic field (NMF) sensing application with design simulations using the model of the ME antenna as a sensor for milliTesla-range magnetic fields.

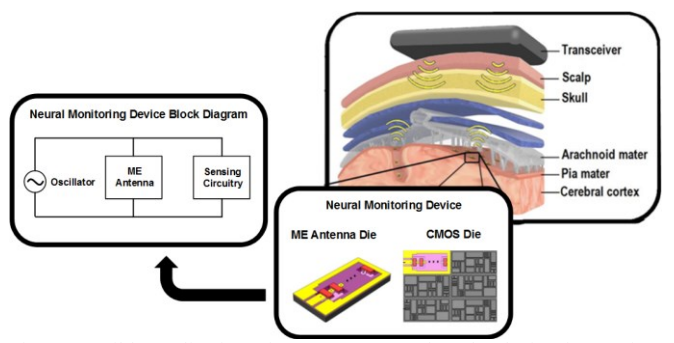


Fig. 1. Possible application of an ME antenna aboard a device for sensing induced neuronal magnetic fields (NMF), which utilizes its amplitude modulation characteristics in the presence of AC magnetic fields.

II. ANALYSIS OF ME ANTENNA BEHAVIOR UNDER AC MAGNETIC FIELDS

A. Sensing Mechanism

Magnetic field sensing is accomplished via a strain response in the ME antenna when exposed to an external magnetic field [3]. Such an external AC magnetic field with amplitude (B_m) and frequency (ω_m) can be described as:

$$B(t) = B_m \cos(\omega_m t) \tag{1}$$

To excite the ME antenna in the sensing mode (NPR), a voltage can be applied to it with an amplitude (V_c) and carrier frequency (ω_c) as follows:

$$V(t) = V_c \cos(\omega_c t) \tag{2}$$

The voltage across the ME antenna due to the ME effect and the nonlinear properties of FeGaB magnetic material (V_{me}) can be expressed as an amplitude modulated signal, where the external AC magnetic field from (1) modulates the carrier voltage from (2):

$$V_{me} = [1 + kB(t)] \cdot mV(t)$$

= $[m + kmB_m \cos(\omega_m t)] \cdot V_c \cos(\omega_c t)$ (3)

In (3), m is the coefficient for the electric field component that is inversely proportional to the thickness of the AlN piezoelectric layer in the ME antenna (t_{AlN}), and k is the magnetoelectric coupling coefficient representing the ME coupling between the antenna and the external AC magnetic field. Note that m is unitless while k has units of Tesla⁻¹.

Equation (3) can be expanded as follows:

$$V_{me} = mV_c \cos(\omega_c t) + \frac{kmB_mV_c}{2} \cos((\omega_c + \omega_m)t) + \frac{kmB_mV_c}{2} \cos((\omega_c - \omega_m)t)$$
(4)

From (4) it can be observed that the modulation components or sidebands are expected to be generated at frequencies $(\omega_c + \omega_m)$ and $(\omega_c - \omega_m)$. The amplitude of these signals is proportional to kB_mV_c according to measurements [3], and thus dependent on the coupling between the magnetic field and the ME antenna. Hence, when demodulated with a carrier, it is possible to determine the frequency content and strength of the magnetic field sensed by the ME antenna [3].

B. Experimental Setup and Measurements

The amplitude modulation during magnetic field sensing has been verified using the setup displayed in Figure 2. The fabricated ME antenna used for measurements has an NPR frequency of 62.23 MHz. Using a lock-in amplifier (Zurich Instruments UHFLI Lock-In Amplifier), this ME antenna was excited in NPR mode (62.23 MHz with an amplitude of 140 mV). The ME antenna is placed inside two Helmholtz coils, the first providing a DC magnetic bias field (in this case, 37 Oe in magnitude) set by the DC current source (Keithley 2461 DC Current Source), and the second providing a test AC magnetic field at a frequency of 1 KHz and with varying amplitudes (B_m) set by the AC current source (Keithley 6221

AC Current Source). Under these conditions the ME antenna exhibits magnetic field sensing behavior.

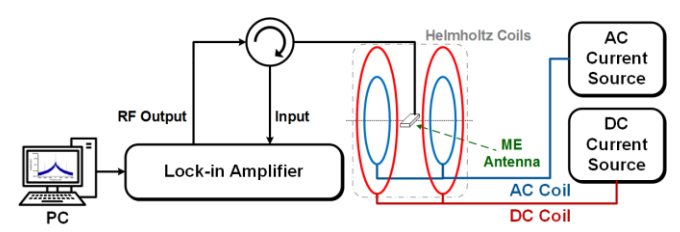
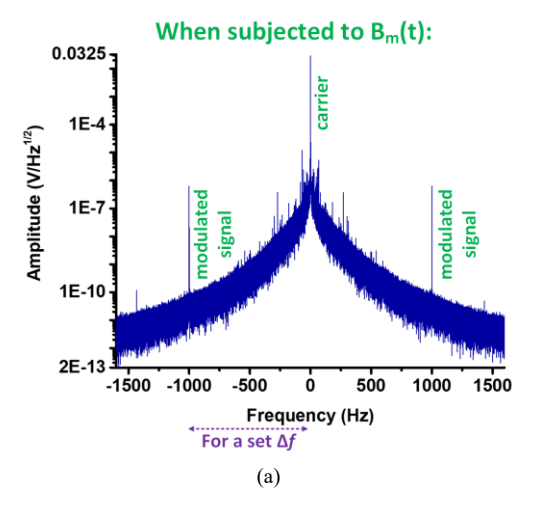


Fig. 2. Block diagram of the experimental setup for ME antenna testing under varying AC magnetic fields.

The lock-in amplifier in Figure 2 receives the returned modulated signal representing the response of the ME antenna. The modulation frequencies are expected to be $(\omega_c + \omega_m)$ and $(\omega_c - \omega_m)$ as seen in the power spectral density plot in Figure 3(a). The change of the modulated voltage (V_{me}) from varying magnetic field strength is plotted in Figure 3(b). Based on measurements, this ME antenna has the capability to sense magnetic fields from as low as 470 pT to more than a milliTesla.



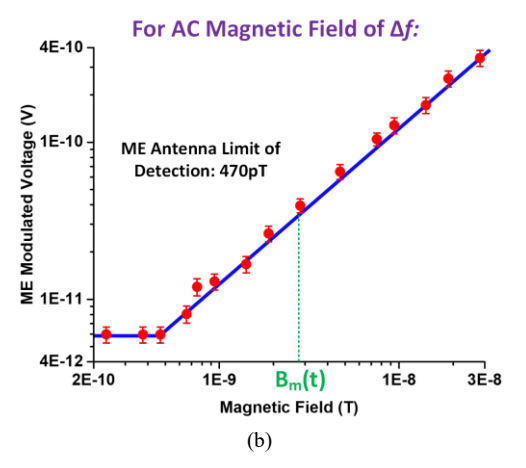


Fig. 3. a) Spectrum of the lock-in amplifier output with a down-converted carrier signal and upper/lower sideband signals. b) Measured modulated output voltage component levels (at 1 KHz) from a sweep of the AC magnetic field magnitude applied to the ME antenna.

III. DYNAMIC CIRCUIT MODEL FOR MAGNETOELECTRIC ANTENNAS

A. Modified Butterworth Van-Dyke Model

The Modified Butterworth Van-Dyke (MBVD) model is commonly utilized to describe the behavior of resonators [12]. It can also be employed to model an ME antenna in the circuit domain, which would allow designers to account for its behavior and performance when designing circuits for magnetic sensing applications. The values of the ideal components (motional parameters R₁, C₁, and L₁, shunt parameters C₀ and R₀, and series resistance R_s) are determined for a particular ME antenna when its Sparameters are measured [12]. The model parameters determined from S-parameter extraction do not change for low magnitudes of AC magnetic fields. As a consequence, this static model does not account for the amplitude modulation behavior of the ME antenna observed in experiments with low magnitudes of AC magnetic fields as discussed in Section II-B. Therefore, the model had to be modified to account for the experimentally observed behavior of the ME antenna, as explained next.

B. Proposed Dynamic Magnetoelectric Antenna Model

The ME antenna being subjected to an external DC magnetic bias field is akin to its "operating point" – as mentioned in Section II-B, the test ME antenna is at its operating point when subjected to a 37 Oe DC magnetic field. The magnitude of the magnetic field was varied from 0-70 Oe, and S-parameter measurements were used to extract component values for the MBVD model [12]. During the experiments, it was observed that the changes in the behavior of the ME antenna can be represented by the variation in the value of parameter L₁ extracted from the measurements under different AC magnetic field strengths, as elaborated in the remainder of this subsection.

The resonance frequency of the ME antenna is highly sensitive to changes in L₁. Since the ME antenna and any additional circuitry are designed for use at a particular NPR frequency, small changes in inductance reflect small changes in the magnetic field environment. The accurate extraction of μ -Tesla field variations around a particular DC bias field is limited by the current MBVD model parameter extraction method. For this reason, a variable inductance was introduced to the model to account for AC magnetic field variations around a DC bias field ("operating point"). The proposed addition of variable inductance to the MBVD model is visualized in Figure 4. This variable inductance (L_{var}) has been implemented using VerilogA to incorporate a timevarying inductance component whose value is a function of the amplitude and frequency of the AC magnetic field and magnetoelectric coupling coefficient (k). Through this modification, a dynamic ME antenna model has been created, which can capture small AC magnetic field changes around the particular operating point (i.e., DC magnetic bias field) during circuit simulations with a conventional simulator (here, Cadence Spectre®). It was verified through AC simulations that the variable model has the same impedance characteristics and resonant frequency as the conventional

MBVD model. Unlike the original static model, the proposed dynamic model can capture the modulation effect in equation (4) during transient simulations. Note that the magnetoelectric coupling coefficient k was adjusted to curve-fit the ME antenna model based on the measurement results. The simulation results with this model are discussed in the following subsection.

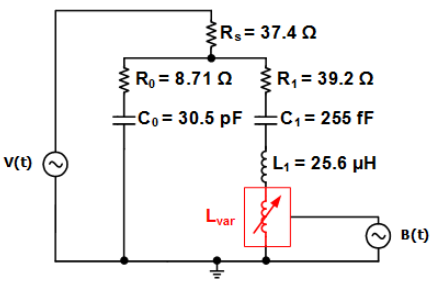


Fig. 4. Proposed dynamic ME antenna model with a time-varying inductance to capture small-signal AC magnetic fields. The annotated values of the components were extracted from S_{11} measurements for a particular ME antenna as mentioned in Section II-B.

C. Simulations of the Dynamic Antenna Model

During simulations, the dynamic ME antenna model was tested using the same conditions as described in Section II-B, with V(t) representing the carrier signal and B(t) representing the AC magnetic field. B(t) was set to a frequency of 1 KHz, and varied over the same range as the measurements (from 0.658nT to 28.2nT). As can be observed in Figure 5, the simulation results with the model agree within 6% error with the measurements for field strengths above 4.5~nT. The deviations at low magnetic field values are influenced by simulator inaccuracies associated with the small modulated voltage levels relative to the large carrier signal.

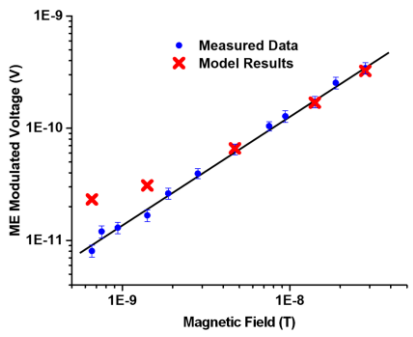


Fig. 5. Comparison of ME antenna model simulation results with measurement results.

IV. ME ANTENNA AS A SENSOR: EXAMPLE DESIGN SIMULATIONS

The presented model of the ME antenna was used for circuit simulations that demonstrate the ME antenna as a sensor of AC magnetic fields when operating in NPR mode. To simulate the ME antenna in sensing mode, it was driven at the NPR resonance frequency (62.23 MHz) as depicted in Figure 6. In this configuration, a square wave clock signal is passed through a passive 4^{th} -order low-pass filter (LPF) with a 62.23 MHz cutoff frequency to smoothen the input waveform at the gate of transistor M_1 that is biased with $I_B =$

 $200~\mu A$. The circuit was designed using a 65nm CMOS technology. In a full implementation, a technique such as the one in [13] can be utilized to generate the high-precision clock signal locked to a high precision source.

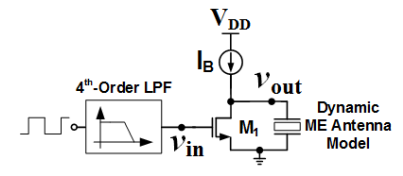


Fig. 6. Example circuit with an ME antenna as a magnetic field sensor.

During simulations, an AC magnetic field input B(t) at 1 KHz was applied to the ME antenna model with varying amplitude. As discussed in Section III, the amplitude modulation is observed across the ME antenna (at V_{out} in Figure 6). Figure 7 displays the sensor's simulated output spectrum for an AC magnetic field amplitude of 2.82 mT. The two components observed at 1 KHz offset around the resonance frequency of 62.23 MHz confirm the sensor simulation capability with the proposed ME antenna model.

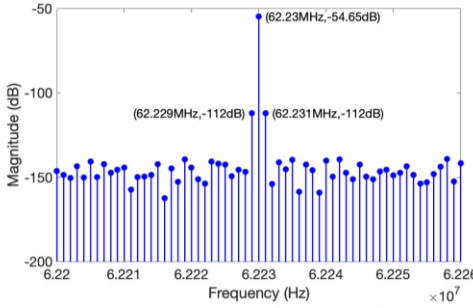


Fig. 7. Sensor output voltage spectrum from a simulation with a magnetic field of 2.82 mT at 1 KHz applied to the ME antenna.

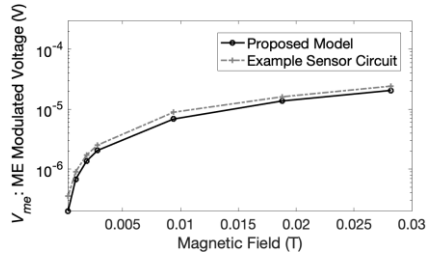


Fig. 8. Modulated voltage component across the ME antenna from simulations with a sweep of the AC magnetic field magnitude of the standalone antenna model (validated through comparison with measurements in Fig. 5), and of the antenna model within the example sensor.

In Figure 8, the modulated voltage across the ME antenna in the example sensor circuit is compared with that from the standalone model simulation (Section III) for different magnetic field amplitudes B(t) between 282 μ T and 28.2 mT. Transient noise of the sensor circuit limits the magnetic field detection for lower values of B(t). Comparing the difference between the levels of the carrier and the modulated signal from the proposed model and the example sensor circuit, the results from these simulations agree within 5% error with the trendline extrapolated from the ME antenna measurements (Figure 5) that were obtained for lower magnetic field amplitudes. This ME antenna application example shows the

usefulness of the dynamic model for design simulations that approximate the sensing characteristics based on the amplitude modulation induced by the magnetic field.

V. CONCLUSIONS

A simulation model for ME antennas was proposed that captures the modulation effect observed when an ME antenna is used to sense low magnetic fields. The dynamic antenna model simulation results showed agreement with the experimental measurement data. Furthermore, the research revealed how the dynamic model can be used for simulations during the design of integrated sensor circuits with ME antennas. Since it provides the first means to estimate output trends, this simulation capability will be utilized to aid the design of complete application-specific magnetic sensor interface circuits with novel ME antennas in the future.

VI. REFERENCES

- [1] Y. Gao, S. Z. Zardareh, X. Yang, T. X. Nan, Z. Y. Zhou, M. Onabajo, M. Liu, A. Aronow, K. Mahalingam, B. M. Howe, G. J. Brown, N. Sun, "Significantly enhanced inductance and quality factor of GHz integrated magnetic solenoid inductors with FeGaB/Al₂O₃ multilayer films," *IEEE Trans. Electron Devices*, vol. 61, no. 5, pp. 1470-1476, May 2014.
- [2] M. Zaeimbashi, H. Lin, C. Dong, X. Liang, M. Nasrollahpour, H. Chen, Ne. Sun, A. Matyushov, Y. He, X. Wang, C. Tu, Y. Wei, Y. Zheng, S. Cash, M. Onabajo, A. Shrivastava, N. Sun, "NanoNeuroRFID: A wireless implantable device based on magnetoelectric antennas," *IEEE J. Electromagnetics, RF, & Microwaves in Medicine & Biology*, vol. 3, no. 3, pp. 206-215, Sept. 2019.
- [3] T. Nan, H. Lin, Y. Gao, A. Matyushov, H. Chen, Ne. Sun, S. Wei, Z. Wang, M. Li, X. Wang, A. Belkessam, R. Guo, B. Chen, J. Zhou, Z. Qian, Y. Hui, M. Rinaldi, M. McConney, B. Howe, Z. Hu, J. Jones, G. Brown, N. Sun, "Acoustically actuated ultra-compact NEMS magnetoelectric antennas," *Nature Communications*, vol. 8, no. 296, pp. 1-8, Aug. 2017.
- [4] J. Wang, X. Chen, "A fluxgate magnetometer for navigation and sensing: Noise character and digital filtering," in *Proc. IEEE Sensors*, Nov. 2015.
- [5] F. Han, S. Harada, I. Sasada, "Fluxgate and search coil hybrid: a low-noise wide-band magnetometer," *IEEE Trans. Magnetics*, vol. 48, no. 11, pp. 3700-3703, Nov. 2012.
- [6] X. Liu, K. H. Lam, K. Zhu, C. Zheng, X. Li, Y. Du, C. Liu, P. Pong, "Overview of spintronic sensors with Internet of Things for smart living," *IEEE Trans. Magnetics*, vol. 55, no.11, Nov. 2019.
- [7] A. Wickens, B. Avants, N. Verma, E. Lewis, J. C. Chen, A. K. Feldman, S. Dutta, J. Chu, J. O'Malley, M. Beierlein, C. Kemere, and J. T. Robinson, "Magnetoelectric materials for miniature, wireless neural stimulation at therapeutic frequencies," retrieved from BioRxiv on 25 May 2020. https://doi.org/10.1101/461855
- [8] M. Suster, N. Vitale, D. Maji, P. Mohseni, "A circuit model of human whole blood in a microfluidic dielectric sensor," *IEEE Trans. Circuits Syst. II: Express Briefs*, vol. 63, no. 12, pp. 1156-1160, Dec. 2016.
- [9] K. Duncan, R. Etienne-Cummings, "A model based approach for realizing a safe wireless biotelemetry system," in *Proc. IEEE Intl. Symp. on Circuits and Systems (ISCAS)*, May 2017.
- [10] M. Stoopman, Y. Liu, H. J. Visser, K. Philips, W. A. Serdijn, "Codesign of electrically short antenna-electronics interfaces in the receiving mode," *IEEE Trans. Circuits Syst. II: Express Briefs*, vol. 62, no. 7, pp. 711-715, July 2015.
- [11] O. Kazanc, F. Maloberti, C. Dehollain, "Simulation oriented rectenna design methodology for remote powering of wireless sensor systems," in *Proc. IEEE Intl. Symp. on Circuits and Systems (ISCAS)*, pp. 2877-2880, May 2012.
- [12] J. Larson, P. Bradley, S. Wartenberg, R. Ruby, "Modified Butterworth-Van Dyke circuit for FBAR resonators and automated measurement system," in Proc. IEEE Ultrasonics Symposium, vol. 1, pp. 863-868, Oct. 2000.
- [13] A. Shrivastava, B. H. Calhoun, "A 150nW, 5ppm,"C, 100kHz on-chip clock source for ultra-low power SoCs," *Proc. Custom Integrated Circuits Conference (CICC)*, 2012.